Inorg. Chem. **2009**, *48*, 4239−4250

Interaction of Copper(II) with the Prion Peptide Fragment HuPrP(76−114) Encompassing Four Histidyl Residues within and outside the Octarepeat Domain

Giuseppe Di Natale,[†] Katalin Ösz,[‡] Zoltán Nagy,[‡] Daniele Sanna,[§] Giovanni Micera,[||] Giuseppe Pappalardo,[⊥] Imre Sóvágó,[*,‡] and Enrico Rizzarelli[*,†,⊥]

Department of Chemical Sciences, University of Catania, Vle A. Doria 6, 95125 Catania, Italy, Institute of Chemistry, University of Debrecen, H-4010 Debrecen, Hungary, Institute of Biomolecular Chemistry, CNR, Traversa La Crucca 3, 07040 Baldinca-Li Punti (Sassari), Italy, Department of Chemistry, University of Sassari, Via Vienna 2, 07100 Sassari, Italy, and Institute of Biostructures and Bioimaging, CNR, Vle A. Doria 6, 95125 Catania, Italy

Received November 14, 2008

Complex formation processes between the 39-mer residue peptide fragment of human prion protein, HuPrP(76−114), and copper(II) ions have been studied by potentiometric, UV−vis, circular dichroism (CD), electron paramagnetic resonance, and electrospray ionization mass spectrometry methods. This peptide consists of 39 amino acid residues and contains two histidines (His77 and His85) belonging to the octarepeat domain and two histidines (His96 and His111) outside this domain. It was found that HuPrP(76−114) is able to bind 4 equiv of metal ions and all histidyl residues are independent, except nonequivalent metal binding sites in the oligonuclear species. Imidazole nitrogen donor atoms are the primary and exclusive metal binding sites below pH 5.5 in the form of various macrochelates. The macrochelation slightly suppresses, but cannot prevent, the deprotonation and metal ion coordination of amide functions, resulting in the formation of (N_{im},N^-), (N_{im},N^-,N^-), and (N_{im},N^-,N^-,N^-)-coordinated copper(II) complexes in the pH range from 5.5 to 9. CD spectroscopy results gave clear evidence for the differences in the metal binding affinity of the histidyl sites according to the following order: His111 > His96 ≫ His77 ∼ His85. Among the oligonuclear complexes, the formation of di- and tetranuclear species seems to be favored over the trinuclear ones, at pH values beyond the physiological ones. This phenomenon was not observed in the complex formation reactions of HuPrP(84−114), a peptide fragment containing only one histidyl residue from the octarepeat. As a consequence, the data support the existence of cooperativity in the metal binding ability of this peptide probably due to the presence of two octarepeat sequences of the dimeric octarepeat domain of HuPrP(76−114) at basic pH values.

Introduction

It has already been widely accepted that a series of neurodegenerative disorders result from abnormalities in the processing of various proteins. Prion diseases are among the best-studied forms of neurodegeneration because they represent a peculiar case in biology because of the widely accepted "protein only" hypothesis, which is based upon the conformational conversion of the normal form of protein (PrP^C) to the disease-related scrapie isoform (PrP^{Sc}).[1,2] The normal physiological function of the prion protein is still a matter of debate, but more and more experimental evidence supports that it is a copper protein that is taking part in the transport or internalization processes of the metal ion.[3−5] A great number of papers have already been published on the complex formation properties of the prion protein as well as of peptide fragments, and the most important findings have already been reviewed.[6−10] It has been widely demonstrated that prion proteins specifically bind copper(II) ions and the

* To whom correspondence should be addressed. E-mail: sovago@delfin.unideb.hu (I.S.), erizzarelli@dipchiunict.it (E.R.). Tel.: +36 52 512900/22303 (I.S.), +39 095 7385070 (E.R.). Fax: +36 52 489667 (I.S.), +39 095 337678 (E.R.).
† University of Catania.
‡ University of Debrecen.
§ Institute of Biomolecular Chemistry, CNR.
|| University of Sassari.
⊥ Institute of Biostructures and Bioimaging, CNR.

(1) Prusiner, S. B. *Proc. Natl. Acad. Sci. U.S.A.* **1998**, *95*, 13363–13383.
(2) Prusiner, S. B. *New England J. Med.* **2001**, *344*, 1516–1526.

10.1021/ic802190v CCC: $40.75
Published on Web 04/06/2009

so-called "octarepeat domain" HuPrP(60−91), containing four well-separated histidyl residues, has been proposed to be the primary metal binding site of the protein.[3] The high metal binding affinity of the octarepeat domain was explained by the involvement of histidyl and adjacent amide residues on the C-terminal side of histidine in metal binding in the form of fused 7- and 5-membered chelate rings.[11−19] However, the full-length protein contains six more histidyl residues outside the octarepeat domain, and two of them, His96 and His111, are located in the unstructured region of the protein. A series of publications support now that prion protein can bind at least six copper(II) ions with the involvement of the octarepeat domain and His96 and/or His111 in metal binding.[20−26]

Our previous studies on the small peptide fragments of prion proteins led to the same conclusions, and the high copper(II) binding affinities of His96,[27] His111,[28] and even His187[29] residues were unambiguously demonstrated. A comparison of the thermodynamic stabilities of the histidine-containing fragments revealed that the peptides modeling the sequences outside the octarepeat domain are even more efficient chelators of copper(II) than the single octarepeat fragments. This difference in the thermodynamic stabilities of histidine-containing peptides was explained by the presence of prolyl residues in the octarepeat fragments. The secondary amide group of the prolyl residue cannot be included in amide binding[30] and, as a consequence, only the (7,5,5)-membered chelates can be formed, while the (6,5,5)-membered fused chelate rings are characteristic of the other histidine-containing fragments. The enhanced stability of the copper(II) complexes is a common feature of all histidine-containing peptides, and it has been exemplified by a great number of literature studies and summarized in reviews.[30,31] These studies well demonstrate the anchoring role of the side-chain imidazole nitrogen donor functions with subsequent metal ion coordination of the deprotonated peptide amide groups on the N-terminal side of the histidyl moieties.

In our most recent paper, we reported the speciation and structures of the complexes formed in the reaction of copper(II) with HuPrP(84−114).[32] This 31 amino acid residue peptide contains three histidines, His85, His96, and His111, thus making possible a comparison of the metal binding affinities of histidyl residues inside and outside the octarepeat domain. Both thermodynamic and spectroscopic data showed the metal ion coordination of all histidyl residues, and this resulted in the existence of coordination isomers in the mononuclear species. The enhanced stability of the copper(II) complex with His111 or His96 residues was obtained over that with His85 representing the monomer of the octarepeat. The formation of di- and trinuclear complexes was found in a relatively high concentration even in equimolar solutions of copper(II) and HuPrP(84−114),[32] showing that the three histidines are independent binding sites, as was reported with several other multihistidine peptides also.[33] The statistical treatment of the speciation curves of these systems led to the conclusion that the formation of polynuclear species in equimolar samples corresponds to the statistical distribution of metal ions among the individual binding sites of ligands, and no cooperativity in metal binding was found, in agreement with recent results that demonstrated a negative cooperativity in the octarepeat

(3) Brown, D. R.; Qin, K. F.; Herms, J. W.; Madlung, A.; Manson, J.; Strome, R.; Fraser, P. E.; Kruck, T. *Nature (London)* **1997**, *390*, 684–687.
(4) Stöckel, J.; Safar, J.; Wallace, A. C.; Cohen, F. E.; Prusiner, S. B. *Biochemistry* **1998**, *37*, 7185–7193.
(5) Westergard, L.; Christensen, H. M.; Harris, D. A. *Biochim. Biophys. Acta* **2007**, *1772*, 629–644.
(6) Millhauser, G. L. *Acc. Chem. Res.* **2004**, *37*, 79–85.
(7) Brown, D. R.; Kozlowski, H. *Dalton Trans.* **2004**, 1907–1917.
(8) Choi, C. J.; Kanthasamy, A.; Anantharam, V.; Kanthasamy, A. G. *NeuroToxicology* **2006**, *27*, 777–787.
(9) Bonomo, P. R.; La Mendola, D.; Pappalardo, G.; Rizzarelli, E.; Sóvágó, I. *Recent Developments in Bioinorganic Chemistry*; M. Saviano: Kerala, India, 2006.
(10) Millhauser, G. L. *Annu. Rev. Phys. Chem.* **2007**, *58*, 299–320.
(11) Viles, J. H.; Cohen, F. E.; Prusiner, S. B.; Goodin, D. B.; Wright, P. E.; Dyson, H. J. *Proc. Natl. Acad. Sci. U.S.A.* **1999**, *96*, 2042–2047.
(12) Burns, C. S.; Aronoff-Spencer, E.; Dunham, C. M.; Lario, P.; Avdievich, N. I.; Antholine, W. E.; Olmstead, M. M.; Vrielink, A.; Gerfen, G. J.; Peisach, J.; Scott, W. G.; Millhauser, G. L. *Biochemistry* **2002**, *41*, 3991–4001.
(13) Marino, T.; Russo, N.; Toscano, M. *J. Phys. Chem. B* **2007**, *111*, 635–640.
(14) Luczkowski, M.; Kozlowski, H.; Stawikowski, M.; Rolka, K.; Gaggelli, E.; Valensin, D.; Valensin, G. *J. Chem. Soc., Dalton Trans.* **2002**, 2269–2274.
(15) Garnett, A. P.; Viles, J. H. *J. Biol. Chem.* **2003**, *278*, 6795–6802.
(16) Chattopadhyay, M.; Walter, E. D.; Newell, D. J.; Jackson, P. J.; Aronoff-Spencer, E.; Peisach, J.; Gerfen, G. J.; Bennett, B.; Antholine, W. E.; Millhauser, G. L. *J. Am. Chem. Soc.* **2005**, *127*, 12647–12656.
(17) Bonomo, R. P.; Cucinotta, V.; Guiffrida, A.; Impellizzeri, G.; Magri, A.; Pappalardo, G.; Rizzarelli, E.; Santoro, A. M.; Tabbi, G.; Vagliasindi, L. I. *Dalton Trans.* **2005**, 150–158.
(18) Valensin, D.; Luczkowski, M.; Mancini, F. M.; Legowska, A.; Gaggelli, E.; Valensin, G.; Rolka, K.; Kozlowski, H. *Dalton Trans.* **2004**, 1284–1293.
(19) Walter, E. D.; Chattopadhyay, M.; Millhauser, G. L. *Biochemistry* **2006**, *45*, 13083–13092.
(20) Burns, C. S.; Aronoff-Spencer, E.; Legname, G.; Prusienr, S. B.; Antholine, W. E.; Gerfen, G. J.; Peisach, J.; Millhauser, G. L. *Biochemistry* **2003**, *42*, 6794–6803.
(21) Jones, C. E.; Abdelraheim, S. R.; Brown, D. R.; Viles, J. H. *J. Biol. Chem.* **2004**, *279*, 32018–32027.
(22) Jones, C. E.; Klewpatinond, M.; Abdelraheim, S. R.; Brown, D. R.; Viles, J. H. *J. Mol. Biol.* **2005**, *346*, 1393–1407.
(23) Belosi, B.; Gaggelli, E.; Guerrini, R.; Kozlowski, H.; Luczkowski, M.; Mancini, F. M.; Remelli, M.; Valensin, D.; Valensin, G. *ChemBioChem.* **2004**, *5*, 349–359.
(24) Berti, F.; Gaggelli, E.; Guerrini, R.; Janicka, A.; Kozlowski, H.; Legowska, A.; Miecznikowska, H.; Migliorini, C.; Pogni, R.; Remelli, M.; Rolka, K.; Valensin, D.; Valensin, G. *Chem.−Eur. J.* **2007**, *13*, 1991–2001.
(25) Klewpatinond, M.; Viles, J. H. *Biochem. J.* **2007**, *404*, 393–402.
(26) Klewpatinond, M.; Viles, J. H. *FEBS Lett.* **2007**, *581*, 1430–1434.
(27) Jószai, V.; Nagy, Z.; Ösz, K.; Sanna, D.; Di Natale, G.; La Mendola, D.; Pappalardo, G.; Rizzarelli, E.; Sóvágó, I. *J. Inorg. Biochem.* **2006**, *100*, 1399–1409.
(28) Di Natale, G.; Grasso, G.; Impellizzeri, G.; La Mendola, D.; Micera, G.; Mihala, N.; Nagy, Z.; Ösz, K.; Pappalardo, G.; Rigó, V.; Rizzarelli, E.; Sanna, D.; Sóvágó, I. *Inorg. Chem.* **2005**, *44*, 7214–7225.
(29) Grasso, D.; Grasso, G.; Guantieri, V.; Impellizzeri, G.; La Rosa, C.; Milardi, D.; Micera, G.; Ösz, K.; Pappalardo, G.; Rizzarelli, E.; Sanna, D.; Sóvágó, I. *Chem.−Eur. J.* **2006**, *12*, 537–547.
(30) Kozlowski, H.; Bal, W.; Dyba, M.; Kowalik-Jankowska, T. *Coord. Chem. Rev.* **1999**, *184*, 319–346.
(31) Sóvágó, I.; Ösz, K. *Dalton Trans.* **2006**, 3841–3854.
(32) Ösz, K.; Nagy, Z.; Pappalardo, G.; Di Natale, G.; Sanna, D.; Micera, G.; Rizzarelli, E.; Sóvágó, I. *Chem.−Eur. J.* **2007**, *13*, 7129–7143.
(33) Kállay, C.; Várnagy, K.; Malandrinos, G.; Hadjiliadis, N.; Sanna, D.; Sóvágó, I. *Dalton Trans.* **2006**, 4545–4552.

region.[19,34] More recently, the interaction of copper(II) with mouse mPrP(23−231) has been reported;[35] the full-length protein resulted in sufficient solubility at pH 7.4 to allow for a spectroscopic [visible circular dichroism (CD) and electron paramagnetic resonance (EPR)] investigation, which demonstrates that the metal binding features in the N-terminus unstructured region, HuPrP(23−125), are largely unaffected by the structured C-terminal domain.[35] In addition, they showed that Cu^{2+} binds to His95 (His96 in humans) preferentially over His110 (His111 in humans) in both the mPrP(91−115) fragment and the full-length mPrP. This preference for the mouse sequence reverses that for the human sequence. On the other hand, it has previously found that the peptide fragment length and pH influence the preference of metal ions over His96 or His111.[25,26] There have been numerous Cu^{2+} binding studies of PrP fragments centered on two regions within the unstructured N-terminal domain of PrP. These studies have separately been focused on the octarepeat region, residues 58−91 or on the region included between the octarepeat and the C-terminal structured domain, between residues 90 and 126. In this work, we report a detailed potentiometric and spectroscopic [UV−vis, CD, EPR, and electrospray ionization mass spectrometry (ESI-MS)] study of the copper(II) complexes with the HuPrP(76−114) prion peptide that contains four histidyl residues, two within and two outside the octarepeat domain. The aim of this investigation is to verify (i) the His111 ability to display the highest affinity of copper(II), which has also recently been questioned,[36] (ii) the presence of cooperativity in this prion peptide containing two histidyl residues within the octarepeat domain, being aware that cooperativity has been shown to be linked to the presence of more than one histidyl residue in the octarepeat region,[15,18] and (iii) the Cu^{2+} coordination modes of the metal complex species formed at different metal-to-ligand ratios, due to the controversy over the Cu^{2+} coordination modes present at intermediate and low copper(II) occupancies.[16,35,37,38]

The study of the copper(II) interaction with this 39 residue peptide fragment represents a necessary step on the way to a detailed thermodynamic and structural characterization of the metal complexes formed by the whole N-terminal unstructured region.

Experimental Section

General Procedures. All *N*-fluorenylmethoxycarbonyl (Fmoc)-protected amino acids, Fmoc-Lys(Boc)-OH, Fmoc-Thr(tBu)-OH, Fmoc-Asn(Trt)-OH, Fmoc-Met-OH, Fmoc-His(Trt)-OH, Fmoc-Ala-OH, Fmoc-Gly-OH, Fmoc-Ser(tBu)-OH, Fmoc-Trp(Boc)-OH, Fmoc-Pro-OH), and Fmoc-Gln(Trt), and 2-(1-*H*-benzotriazol-1-yl)-1,1,3,3-tetramethyluronium tetrafluoroborate (TBTU) were obtained from Novabiochem (Switzerland); Fmoc-PAL-PEG resin, *N*,*N*-diisopropylethylamine (DIEA), *N*,*N*-dimethylformamide (DMF, peptide synthesis grade), and a 20% piperidine−DMF solution were from Applied Biosystems; *N*-hydroxybenzotriazole (HOBT), triisopropylsilane (TIS), trifluoroacetic acid (TFA), and ethanedithiol (EDT) were purchased from Sigma/Aldrich. All other chemicals were of the highest available grade and were used without further purification.

Preparative reversed-phase high-performance liquid chromatography (rp-HPLC) was carried out by means of a Varian PrepStar 200 model SD-1 chromatography system equipped with a Prostar photodiode array detector with detection at 222 nm. Purification was performed by eluting with solvent A (0.1% TFA in water) and solvent B (0.1% TFA in acetonitrile) on a Vydac C_{18} 250 × 22 mm (300 Å pore size; 10−15 μm particle size) column. Analytical rp-HPLC analyses were performed using a Waters 1525 instrument, equipped with a Waters 2996 photodiode array detector with detection at 222 nm.

The peptide samples were analyzed using gradient elution with solvents A and B on a Vydac C_{18} 250 × 4.6 mm (300 Å pore size; 5 μm particle size) column.

Synthesis of the Peptide HuPrP(76−114). HuPrP(76−114) was assembled using the solid-phase peptide synthesis strategy on a Pioneer peptide synthesizer. All residues were introduced according to the TBTU/HOBT/DIEA activation method for Fmoc chemistry on Fmoc-PAL-PEG resin (substitution 0.180 mmol/g, 0.270 mmol scale synthesis, 1.5 g of resin). The synthesis was carried out under a 4-fold excess of amino acid at every cycle, and each amino acid was recirculated through the resin for 35 min. Removal of Fmoc protection during the synthesis was achieved by means of a 20% piperidine solution in DMF. N-Terminal acetylation was performed by treating the fully assembled and protected peptide resins (after removal of the N-terminal Fmoc group) with a solution containing acetic anhydride (6% v/v) and DIEA (5% v/v) in DMF.

The peptide was cleaved from the resin and simultaneously deprotected by treatment with a mixture of TFA/TIS/EDT/H_2O (94.0/1.0/2.5/2.5% v/v) for 2 h at room temperature. The solution containing the free peptide was filtered from the resin and concentrated in vacuo at 30 °C. The peptide was precipitated with cold freshly distilled diethyl ether. The precipitate was then filtered, dried under vacuum, redissolved in water, and lyophilized. The resulting crude peptide was purified by preparative rp-HPLC.

HuPrP(76−114) was purified by preparative rp-HPLC on a Vydac C_{18} chromatographic column at a flow rate of 20 mL/min, using the following instrumental conditions: isocratic elution at 13% B from 0 to 8 min, then a linear gradient from 13 to 20% B over 20 min, and finally isocratic elution at 20% B from 20 to 30 min (R_t = 24 min). The purity of the peptide was checked by analytical rp-HPLC using a Vydac C_{18} chromatographic column at a flow rate of 1 mL/min, with isocratic elution at 5% B, then a a linear gradient from 5 to 30% B over 18 min, and finally isocratic alution at 30% B from 18 to 30 min (R_t = 19 min). The purity of the peptide was greater than 98%, and the yield was 45%. The product was characterized by ESI-MS: *m*/*z* 2036.9 $[M + 2H]^{2+}$, 1358.3 $[M + 3H]^{3+}$, 1018.7 $[M + 4H]^{4+}$, 814.8 $[M + 5H]^{5+}$, 678.9 $[M + 6H]^{6+}$, 583.4 $[M + 7H]^{7+}$. Calcd for $C_{177}H_{258}N_{60}O_{49}S_2$: *m*/*z* 4071.9.

Potentiometric Measurements. The pH−potentiometric titrations were carried out in 3 mL samples in the concentration range 1×10^{-3}−4×10^{-3} mol dm^{-3}, with the metal ion-to-ligand ratios between 1:1 and 5:1. During the titration, argon was bubbled through the samples to ensure the absence of oxygen and carbon dioxide and also to stir the solutions. All titrations were performed

(34) Tompsett, A. R.; Abdelraheim, S. R.; Daniels, M.; Brown, D. R. *J. Biol. Chem.* **2005**, *280*, 42750–42758.
(35) Klewpatinond, M.; Davies, P.; Bowen, S.; Brown, D. R.; Viles, J. H. *J. Biol. Chem.* **2008**, *283*, 1870–1881.
(36) Treiber, C.; Thompsett, A. R.; Pipkorn, R.; Brown, D. R.; Multhaup, G. *J. Biol. Inorg. Chem.* **2007**, *12*, 711–720.
(37) Wells, M. A.; Jelinska, C.; Hosszu, L. L. P.; Craven, C. J.; Clarke, A. R.; Collinge, J.; Waltho, J. P.; Jackson, G. S. *Biochem. J.* **2006**, *400*, 501–510.
(38) Wells, M. A.; Jackson, G. S.; Jones, S.; Hosszu, L. L. P.; Craven, C. J.; Clarke, A. R.; Collinge, J.; Waltho, J. P. *Biochem. J.* **2006**, *399*, 435–444.

at 298 K and at a constant ionic strength of 0.2 mol dm^{-3} (KCl) with a pH-meter radiometer pHM84 equipped with a 6.0234.100 combination glass electrode (Metrohm) and a Dosimat 715 automatic buret (Metrohm) containing carbonate-free potassium hydroxide in a known concentration. The pH readings were converted into hydrogen ion concentration and protonation constants of the ligands, and the overall stability constants (log β_{pqr} for $M_pH_qL_r$) of the complexes were calculated by means of a general computational program, *Hyperquad*,[39] using eqs 1 and 2.

$$pM + qL + rH = M_pL_qH_r \quad (1)$$

$$\beta_{pqr} = \frac{[M_pL_qH_r]}{[M]^p[L]^q[H]^r} \quad (2)$$

Stock solutions of potassium hydroxide (used as a titrant for the potentiometric studies), potassium chloride (used to keep the ionic strength constant, at 0.2 mol dm^{-3}), and copper(II) chloride were prepared from analytical-grade reagents. The concentration of the base was checked by conventional potentiometric titrations, while that of copper(II) chloride was checked gravimetrically via the precipitation of oxinate.

Further details of the potentiometric studies and equilibrium analysis of systems containing large peptide fragments have already been reported in our previous publication.[32]

Spectroscopic Studies. UV−vis spectra (300−900 nm) were recorded at 25 °C on a Perkin-Elmer Lambda 35 spectrophotometer using 1-cm-path-length quartz cells. The concentrations of the peptide and copper(II) used to record absorption spectra were the same as those for the potentiometric titrations.

CD spectra were obtained at 25 °C under a constant flow of nitrogen on a Jasco model J-810 spectropolarimeter, which was calibrated with an aqueous solution of (1*R*)-(−)-10-camphorsulfonic acid. Measurements were carried out in water at different pH values, using 1-mm- or 1-cm-path-length cuvettes. The CD spectra of the copper(II) complexes were obtained in the wavelength ranges of both 200−400 and 300−800 nm, respectively. All of the solutions were freshly prepared using deionized water. The concentrations of the peptide and copper(II) used for the acquisition of the CD spectra in the visible region were identical with those of the potentiometric titrations, whereas far-UV CD spectra were recorded using concentrations of the peptide and copper(II) ranging between 2×10^{-4} and 2×10^{-5} mol dm^{-3}.

Frozen-solution EPR spectra were recorded on a Bruker EMX spectrometer at 120 K. Copper(II) complex solutions (1×10^{-3} mol dm^{-3}) were prepared by dissolving in the necessary volume of a standard solution of $^{63}CuSO_4$ the appropriate amount of the peptide ligand ranging from 1:1 to 4:1 metal-to-ligand ratios and adjusting the pH of the resulting solution to the desired value by adding 10^{-2} mol dm^{-3} KOH or H_2SO_4. Copper(II) stock solutions for EPR measurements were prepared from $CuSO_4 \cdot 5H_2O$, which had been enriched with ^{63}Cu to achieve a better resolution of EPR spectra. Metallic copper (99.3% ^{63}Cu and 0.7% ^{65}Cu) was purchased from JV Isoflex (Moscow, Russia) for this purpose and converted into the sulfate. Ethylene glycol (10%) was added to the aqueous copper(II) complex solutions to increase the resolution and to avoid aggregation processes.

ESI-MS spectra were recorded on a Finnigan LCQ-DECA ion-trap electrospray mass spectrometer (Bremen, Germany). Peptide solutions were introduced into the ESI source via a 100-μm-i.d. fused-silica column, using a 250 μL syringe. The experimental conditions for spectra acquired in positive-ion mode were as follows: needle voltage 2.5 kV; flow rate 5 μL/min; source temperature 300 °C; *m/z* range 200−4000; cone potential 46 V; tube lens offset −10 V. The complexes were prepared by dissolving the peptide (5×10^{-5} mol dm^{-3}) and $CuSO_4$ in Milli-Q water at 1:1−5:1 Cu^{II}/L ratios and investigated in the 4.0−10.0 pH range, adjusting the pH values by adding HCl or NaOH.

Table 1. Overall Protonation Constants (log β_{pqr})[a] and Stepwise pK_a Values of the Peptide HuPrP(76−114) at $T = 298$ K and $I = 0.2$ mol dm^{-3} KCl

species	log β_{pqr}	pK_a
$[HL]^+$	11.16(10)	11.16
$[H_2L]^{2+}$	21.59(5)	10.43
$[H_3L]^{3+}$	31.57(4)	9.98
$[H_4L]^{4+}$	40.71(3)	9.14
$[H_5L]^{5+}$	47.67(2)	6.96
$[H_6L]^{6+}$	54.05(2)	6.38
$[H_7L]^{7+}$	60.07(2)	6.02
$[H_8L]^{8+}$	65.43(3)	5.36

[a] Standard deviations are in parentheses.

Results and Discussion

Proton Complex Formation. Protonation constants of the 39 amino acid residue peptide, HuPrP(76−114), have been determined by potentiometric titrations, and the data are collected in Table 1. It is clear from Table 1 that the ligand contains eight protonation sites, which correspond to four lysyl (Lys101, Lys104, Lys106, and Lys110) and four histidyl (His77, His85, His96, and His111) residues. In agreement with the behavior of the previously investigated peptide fragments of prion,[27−29] it is evident that deprotonations of the lysyl ammonium groups take place in a high pH range (pH ∼9−11), while those of the imidazolium groups occur in the pH 5−7 range. The average pK_a values of the lysyl amino and histidyl imidazole groups are 10.18 and 6.18, respectively, indicating that the deprotonation reactions of both lysine and histidine side chains take place in overlapping processes. Similar considerations were reported for the HuPrP(84−114) peptide containing three histidyl residues.[32] In the cases of tri-, tetra-, and pentapeptides containing several histidine amino acids, the microscopic protonation constants have also been determined by NMR measurements, and an almost complete independence of the protonation reactions of the separate histidyl residues was obtained.[40] It was also demonstrated that small differences in the microscopic protonation constants of the histidyl residues can be obtained if these residues are present in terminal positions or in the close vicinity of another acidic (e.g., carboxylic) group. In the case of HuPrP(76−114), all protonation sites are separated from the N or C termini and no other donor functions are present in the molecule, supporting the high similarity of the microscopic protonation constants of lysyl and histidyl residues.

Copper(II) Complex Speciation and Coordination Environment Features. Stability constants of the copper(II) complexes of HuPrP(76−114) have been determined by potentiometric measurements at five different metal ion-to-

(39) Gans, P.; Sabatini, A.; Vacca, A. *Talanta* **1996**, *43*, 1739–1753.

(40) Kállay, C.; Ösz, K.; Dávid, A.; Valastyán, Z.; Malandrinos, G.; Hadjiliadis, N.; Sóvágó, I. *Dalton Trans.* **2007**, 4040–4047.

Table 2. Stability Constants (log β_{pqr})[x] of the Copper(II) Complexes of the Peptide HuPrP(76−114) at $T = 298$ K and $I = 0.2$ mol dm^{-3} KCl

mononuclear species		dinuclear species	
species	log β_{pqr}	species	log β_{pqr}
$[CuH_7L]^{9+}$	64.59(5)	$[Cu_2H_4L]^{8+}$	52.96(5)
$[CuH_6L]^{8+}$	60.28(3)	$[Cu_2H_3L]^{7+}$	47.08(4)
$[CuH_5L]^{7+}$	54.90(4)	$[Cu_2H_2L]^{6+}$	41.20(5)
$[CuH_4L]^{6+}$	49.55(2)	$[Cu_2HL]^{5+}$	34.81(4)
$[CuH_3L]^{5+}$	42.95(2)	$[Cu_2L]^{4+}$	27.55(5)
$[CuH_2L]^{4+}$	35.86(2)	$[Cu_2H_{-1}L]^{3+}$	20.20(3)
$[CuHL]^{3+}$	27.98(1)	$[Cu_2H_{-2}L]^{2+}$	12.03(3)
$[CuL]^{2+}$	18.75(2)	$[Cu_2H_{-3}L]^{+}$	2.84(3)
$[CuH_{-1}L]^{+}$	8.98(2)	$[Cu_2H_{-4}L]$	−7.03(3)
$[CuH_{-2}L]$	−1.50(3)	$[Cu_2H_{-5}L]^{-}$	−17.32(4)
$[CuH_{-3}L]^{-}$	−12.15(3)	$[Cu_2H_{-6}L]^{2-}$	−28.08(4)
$[CuH_{-4}L]^{2-}$	−23.81(4)	$[Cu_2H_{-7}L]^{3-}$	−39.42(5)
		$[Cu_2H_{-8}L]^{4-}$	−51.01(6)
trinuclear species		tetranuclear species	
species	log β_{pqr}	species	log β_{pqr}
$[Cu_3HL]^{7+}$	38.11(6)	$[Cu_4H_{-3}L]^{5+}$	15.80(8)
$[Cu_3L]^{6+}$	32.10(5)	$[Cu_4H_{-4}L]^{4+}$	9.46(5)
$[Cu_3H_{-1}L]^{5+}$	25.85(4)	$[Cu_4H_{-5}L]^{3+}$	2.30(4)
$[Cu_3H_{-2}L]^{4+}$	18.75(5)	$[Cu_4H_{-6}L]^{2+}$	−5.52(3)
$[Cu_3H_{-3}L]^{3+}$	11.23(5)	$[Cu_4H_{-7}L]^{+}$	−14.11(4)
$[Cu_3H_{-4}L]^{2+}$	2.61(7)	$[Cu_4H_{-8}L]$	−23.32(4)
		$[Cu_4H_{-9}L]^{-}$	−32.96(5)
		$[Cu_4H_{-10}L]^{2-}$	−43.17(5)
		$[Cu_4H_{-11}L]^{3-}$	−53.79(6)
		$[Cu_4H_{-12}L]^{4-}$	−64.54(6)
		$[Cu_4H_{-13}L]^{5-}$	−76.02(7)
		$[Cu_4H_{-14}L]^{6-}$	−87.70(10)

[x] Standard deviations are in parentheses.

ligand ratios changing from 1:1 to 5:1. The formation of a copper(II) hydroxide precipitate above pH 6 was observed only in the latter case (at 5:1 metal-to-ligand ratio), suggesting that mono- to tetranuclear species can exist in solution even at high pH values. The formation of at least 43 different species was taken into account in the final model of the computer evaluation of the system, and their stability constants are collected in Table 2. The high number of different species made it necessary to record CD, UV−vis, and EPR spectra of the system at four different metal ion-to-ligand ratios in a wide pH range ($4 \leq pH \leq 11$) in all cases. The combined experimental and mathematical treatment of such a complicated equilibrium system has already been reported in our previous paper on the example of the copper(II)−HuPrP(84−114) system.[32] It was concluded that, for this ligand, all histidines were independent metal binding sites resulting in the existence of mono- to trinuclear complexes. The equilibrium and spectroscopic results obtained for the copper(II)−HuPrP(76−114) system support a similar behavior, but the presence of the fourth histidine makes the formation of tetranuclear species also possible.

Figures 1 and 2 demonstrate the metal ion speciation in equimolar samples and at 3:1 copper(II)-to-ligand ratios. The high number of species in Table 2 rules out the correct description of the traditional pH-dependent speciation curves. It is clear, however, that the mononuclear species dominate in the equimolar samples and they are plotted separately, while the dinuclear species are given as the total of the concentration of all dinuclear species in different protonation stages. In Figure 2, at a 3:1 copper(II)-to-ligand ratio, the thin lines represent the 43 species that can be calculated from

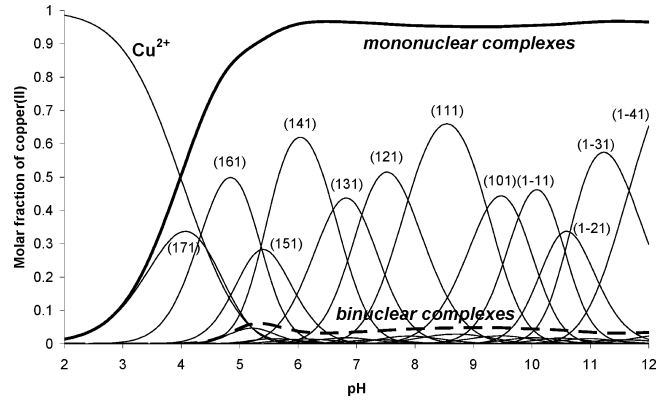

Figure 1. Concentration distribution of the various species formed in the copper(II)−HuPrP(76−114) system at equimolar samples. $c_{copper(II)} = c_L = 1 \times 10^{-3}$ mol dm^{-3}. The numbers used for the identification of different species refer to *pqr* in $Cu_pH_qL_r$, e.g., $CuH_2L = 121$. The bold line indicates the sum of the mononuclear complex species containing a single copper(II) ion bound to the ligand (see Scheme 1a,c−e). The dashed line indicates the sum of the binuclear complex species containing two copper(II) ions bound to the ligand (see Scheme 1b,g).

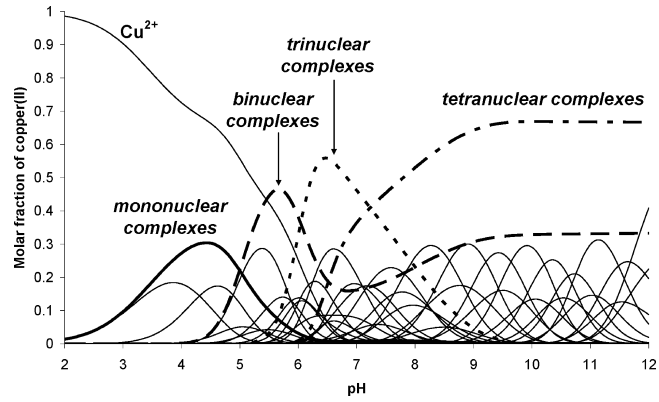

Figure 2. Concentration distribution of the various species formed in the copper(II)−HuPrP(76−114) system at a 3:1 metal ion-to-ligand ratio. $c_{copper(II)} = 3 \times 10^{-3}$ mol dm^{-3}, and $c_L = 1 \times 10^{-3}$ mol dm^{-3}. The bold line indicates the sum of the mononuclear complex species containing a single copper(II) ion bound to the ligand (see Scheme 1a,c−e). Then different types of dashed lines indicate the sum of the bi-, tri-, and tetranuclear complex species containing respectively two (see Scheme 1b,g), three (see Scheme 1f), and four (see Scheme 1h) copper(II) ions bound to the ligand.

the data of Table 2, while the thick dotted lines show the sum of the overall concentrations of the complexes with different numbers of copper(II) ions. The plots of the 43 different species are used to demonstrate only the complexity of the system, but the major conclusion can be drawn from the overall concentrations of the mono- to tetranuclear species.

Because of the presence of four lysyl residues in the peptide, both mono- and oligonuclear species can exist in many different protonation stages. For example, the stoichiometries of the mononuclear complexes vary from $[CuH_7L]^{9+}$ to $[CuH_{-4}L]^{2-}$, suggesting the existence of several different binding modes in different pH ranges. In agreement with this expectation, a continuous change of UV−vis, CD, and EPR spectra of the system can be observed by increasing the pH, supporting the involvement of more and more (up to four) nitrogen donors in copper(II) binding. Our previous studies on the peptide fragments of prion protein came to the conclusion that amino groups of lysyl residues are not

Scheme 1. Binding Modes of the Major Species Formed in the Copper(II)−HuPrP(76−114) System at Different Metal Ion-to-Ligand Ratios by Increasing the pH[a]

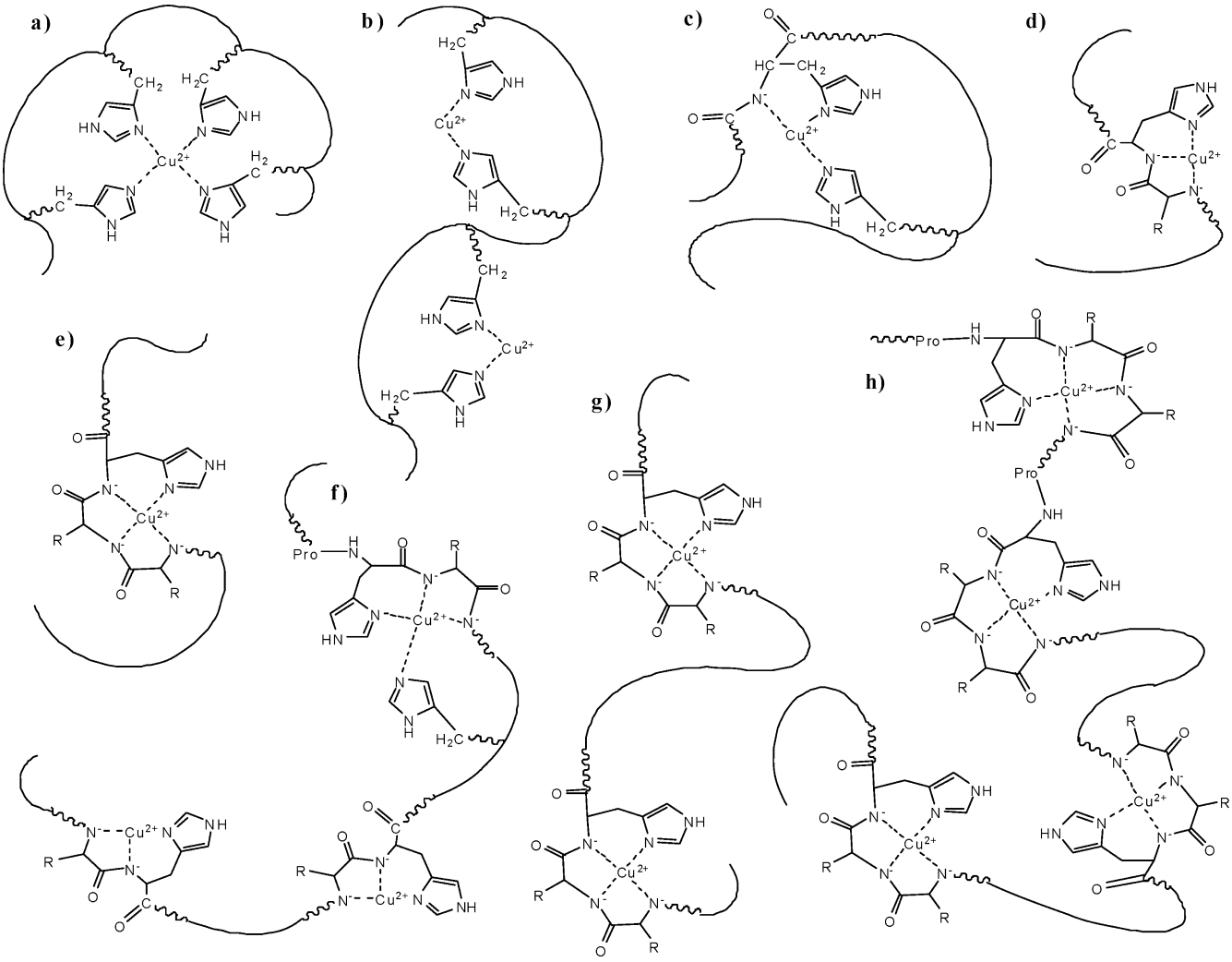

[a] The binding modes a, d, and e indicate mononuclear complex species. The binding modes b and g indicate dinuclear complex species. The binding mode f indicates a trinuclear complex species. The binding mode h indicates a tetranuclear complex species. Binding modes: (a) 4N macrochelate (e.g., $[CuH_4L]^{6+}$ predominating in equimolar samples at pH 6); (b) 2N macrochelates in dinuclear species (e.g., $[Cu_2H_4L]^{8+}$ existing at high metal-to-ligand ratios at pH 6); (c) (N_{im},N^-,N_{im}) coordination (e.g., $[CuH_3L]^{5+}$ present around the pH in the overlap with several other species); (d) (N_{im},N^-,N^-) coordination (e.g., $[CuH_2L]^{4+}$ present in the pH 7−8 range in the overlap with several other 2N, 3N, and 4N complexes); (e) (N_{im},N^-,N^-,N^-) coordination (e.g., from $[CuHL]^{3+}$ to $[CuH_{-3}L]^-$ predominating species above pH 8); (f) 3N-coordinated trinuclear complexes (e.g. $[Cu_3H_{-2}L]^{4+}$ present at 3:1 or 4:1 metal-to-ligand ratios in the pH 6−8 range); (g) 4N-coordinated dinuclear complex (e.g., from $[Cu_2H_{-2}L]^{2+}$ to $[Cu_2H_{-6}L]^{2-}$ predominating species at 2:1 and 3:1 ratios above pH 8); (h) 4N-coordinated tetranuclear complex (e.g., from $[Cu_4H_{-8}L]$ to $[Cu_4H_{-12}L]^{4-}$ predominating species at 3:1 and 4:1 ratios above pH 8).

metal-binding sites under any circumstances.[28,32] Spectroscopic measurements on the copper(II)−HuPrP(76−114) system are in line with the same results because the deprotonation processes above pH 10 are not accompanied by any spectral changes. From these data, we can assume that all lysine residues are in the protonated form, at least below pH 9. As a consequence, the protonated complexes from $[CuH_7L]^{9+}$ to $[CuH_4L]^{6+}$ contain four protonated lysyl ammonium groups, and even some of the imidazoles are present in protonated forms in the acidic pH range. The stoichiometries of these species unambiguously rule out the involvement of amide nitrogens in metal binding below pH 5.5, and this is supported by the lack of any measurable CD activity of the samples below this pH.

Copper(II) binding sites of the species $[CuH_7L]^{9+}$ to $[CuH_4L]^{6+}$ can be described with the involvement of one to four imidazole nitrogen atoms in coordination. Taking into account the protonation constants of lysyl residues, the equilibrium parameters of Cu−N_{im}-bonded complexes can be calculated, and these values, together with some spectral data, are collected in Table 3. The increase of log K values and the continuous blue shift of absorption spectra by increasing the pH suggest that all deprotonated imidazole nitrogens are metal binding sites in the form of macrochelates. The relatively low concentration of the various species and especially the significant overlap in their formation do not make it possible to calculate individual spectral param-

Table 3. Calculated Stepwise Stability Constant Values (log K) and Spectral Data of Cu−N_{im}-Coordinated Species

pH	major species	binding mode	log K	λ_{max} (nm)
4.0	$[CuH_7L]^{9+}$	Cu−$1N_{im}$	4.52	780
4.8	$[CuH_6L]^{8+}$	Cu−$2N_{im}$	6.23	660
5.3	$[CuH_5L]^{7+}$	Cu−$3N_{im}$	7.23	640
6.0	$[CuH_4L]^{6+}$	Cu−$4N_{im}$	8.84	625

eters of the different species. The comparison of these values with those reported for the macrochelates of simple multihistidine peptides in our previous publication,[33] however, reveals a high similarity in both thermodynamic and spectral data. It is also clear from this comparison that the peptide HuPrP(76−114) is especially well suited for macrochelation because the log K values of the $2N_{im}$- and $3N_{im}$-coordinated complexes are slightly higher than those of HuPrP(84−114) or the HisXaaHisXaaHis pentapeptides.[33] The $[CuH_4L]$ species, that is, the main complex formed at pH 6 (Figure 1, indicated by 141), shows a stability constant (log $K = 8.84$; Table 3) higher than that reported for the analogous species formed by the tetraoctarepeat peptide (log $K = 8.60$).[18] The high difference in the charge of the two species and the different experimental conditions make it difficult to compare the two values, but we can conclude that the affinity of HuPrP(76−114) to form four histidine macrochelate (two within and two outside the octarepeat region; Scheme 1a) is at least on the same order of magnitude as that reported for the multiple histidine-coordinated residues included in the tetraoctarepeat of the prion protein. There are, however, significant differences in the spectral parameters of the species. Namely, $\lambda_{max} = 588$ and 625 nm, $A_{||} = 195 \times 10^{-4}$ and 174×10^{-4} cm^{-1}, and $g_{||} = 2.24$ and 2.28 were obtained for the $4N_{im}$ macrochelates of HuPrP(60−91)[18] and HuPrP(76−114), respectively. These values suggest a high distortion from the planarity in the case of the copper(II) complex of HuPrP(76−114) and seem to support the stabilizing role of proline residues in macrochelation, that is, a conformation of the ligand more suitable for this purpose.

An important difference in the speciation curves of copper(II)−HuPrP(84−114) and −HuPrP(76−114) systems is linked to the total amount and the pH range of the formation of oligonuclear complexes. In the case of HuPrP(84−114), the dinuclear complexes formed parallel with the deprotonation of amide functions and the macrochelation prevented the monodentate imidazole binding in oligonuclear species.[33] However, it is clear from Table 2 that the species $[Cu_2H_4L]^{8+}$ is also present in the copper(II)−HuPrP(76−114) system. Taking into account the four protonated lysyl side chains, copper(II) ions can coordinate only separate imidazole nitrogen donor atoms in this species. The lack of such a species in the copper(II)−HuPrP(84−114) system indicates that its formation requires the presence of four imidazole moieties and they can coordinate both copper(II) ions in the form of $2N_{im}$ macrochelates (Scheme 1b). The log K value for the reaction of two Cu^{2+} with H_4L is 12.25, and 6 log units is a common value for the formation of $2N_{im}$ macrochelates. However, it should be clarified that $[Cu_2H_4L]^{8+}$ is not a major species at any metal ion-to-ligand ratios, and the $4N_{im}$ macrochelate (see Scheme 1a) predominates if the metal ion and ligand are present in comparable concentrations.

The binding modes of the species from $[CuH_3L]^{5+}$ to $[CuH_{-4}L]^{2-}$ can be described by the involvement of deprotonated amide functions in metal ion coordination. It is clear from Figure 1 that the deprotonation reactions take place in successive reactions and all species are present in measurable concentration. It is a significant difference from the small peptide fragments containing only one histidyl residue, where the deprotonation of two adjacent amide functions took place in a cooperative manner and the species with (N_{im},N^-) coordination mode were present in negligible concentration.[27,28,31] On the contrary, the deprotonation patterns of the copper(II)−HuPrP(84−114) and −HuPrP(76−114) systems are quite similar to each other, suggesting that distant histidyl residues can stabilize the intermediate species with (N_{im},N^-,N_{im}) binding mode containing a 6-membered chelate and a macrochelate (see Scheme 1c). The pK_a values for the subsequent deprotonation reactions of one, two, and three amide groups are 6.60, 7.09, and 7.88, respectively. The first two values are slightly higher than those reported for the small peptide fragments,[27−29] indicating that the macrochelation slightly suppresses the formation of amide-bonded species. This effect is, however, rather weak and cannot prevent the formation of the (N_{im},$2N^-$)-coordinated complexes (see Scheme 1d).

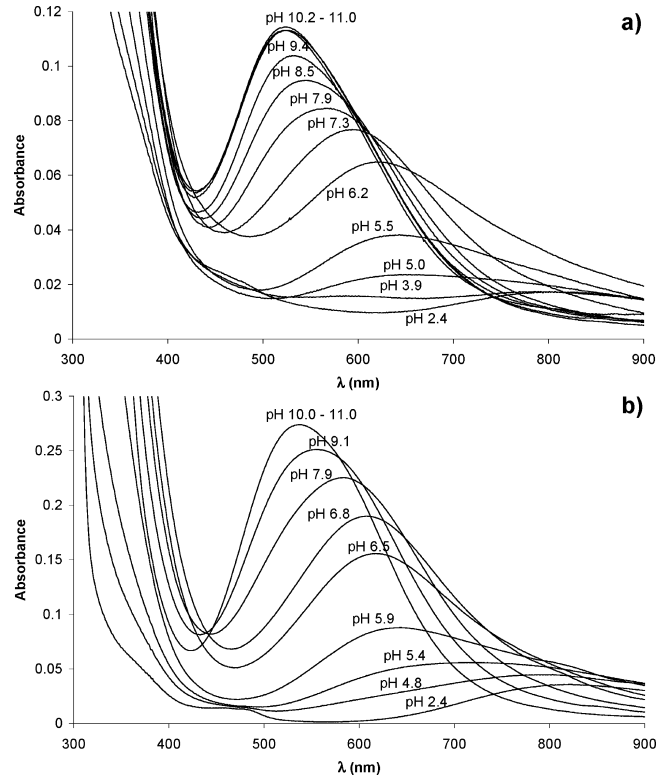

Figure 3. Visible absorption spectra of the copper(II) complexes of HuPrP(76−114) at different metal ion-to-ligand ratios and pH values: (a) 1:1 ratio, $c_{copper(II)} = 0.85 \times 10^{-3}$ mol dm^{-3}, $c_L = 0.85 \times 10^{-3}$ mol dm^{-3}; (b) 3:1 ratio, $c_{copper(II)} = 2.6 \times 10^{-3}$ mol dm^{-3}, $c_L = 0.81 \times 10^{-3}$ mol dm^{-3}.

The above-mentioned conclusions were based upon the equilibrium data, but they are also well supported by the spectroscopic measurements. First of all, the deprotonation and metal ion coordination of the amide functions are accompanied by a significant blue shift of the absorption spectra, as is demonstrated by Figure 3. The high number and the significant overlap of the species rule out the calculation of the individual parameters, but the range of the absorption maxima corresponds well to those of the 2N

or 3N complex species. For example, the species $[CuH_2L]^{4+}$ (=$[CuH_{-2}LH_4]^{4+}$ corresponds to a 3N complex, and its concentration reaches a maximum of around pH 7.5, where the absorption maxima of the d−d bands occur at $\lambda = 600$ nm, which is a common value for this type of coordination. The species $[CuHL]^{3+}$ predominates in the pH 8−9 range (see Figure 1), and its spectral parameters are in good agreement with those of other (N_{im},$3N^-$)-coordinated complexes (Scheme 1e) [$\lambda_{max} = 520-530$ nm, $\epsilon = 117$ M^{-1} cm^{-1}, $A_{||} = (200-202) \times 10^{-4}$ cm^{-1}, and $g_{||} = 2.193-2.196$]. These data reveal that we can give only a narrow range and not a fixed value for the spectroscopic parameters of $[CuHL]^{3+}$ because several coordination isomers of the amide-bonded species can exist. The (N_{im},N^-), (N_{im},$2N^-$) and (N_{im},$3N^-$) coordination modes can be formed with any of the four histidines of HuPrP(76−114). Previous studies on the small peptide fragments revealed that their thermodynamic stability and UV−vis and EPR spectral parameters are rather similar to each other and cover the range given above for the 4N-coordinated complexes. Of course, the different amino acid sequences in the vicinity of His96, His111, and the octarepeat histidines result in some small changes in the characteristic parameters, but these differences are too small to be detected in a multicomponent system. The measured visible and EPR spectra of the coordinatively saturated copper(II) complexes are, however, not exactly the same at different metal-to-ligand ratios, suggesting that the molar ratio of coordination isomers is not the same, similar to the copper(II)−HuPrP(84−114) system.

Visible CD spectra of the 3N and 4N complexes are largely affected by the amino acids present in the vicinity of histidyl residues and can be used to assess the relative abundance of various coordination isomers. The mathematical treatment of CD spectra has already been demonstrated in our previous paper on the example of the copper(II)−HuPrP(84−114) system.[32] This molecule contains His85, His96, and His111 residues, and the CD spectra of their 3N and 4N complexes are significantly different because the amino acids of the sequences HGG, GTH, and MKH are involved in metal binding, respectively. In the case of HuPrP(76−114), the peptide contains one more octarepeat monomers. As a consequence, we cannot distinguish between the metal ion occupancies of the two octapeptide fragments, but their relationship to the histidines outside the octarepeat domain can be assessed. Figure 4 is used to demonstrate the differences of the CD spectra obtained at 1:1 and 3:1 metal ion-to-ligand ratios and different pH values (see the Supporting Information for the visible CD spectra of the 2:1 and 4:1 metal ion-to-ligand ratios). It is clear that the highest differences can be observed between the 1:1 and 2:1 metal-to-ligand ratios, and it is also clear that CD spectra of HuPrP(76−114) are quite similar to those of HuPrP(84−114) obtained under the same conditions. The main differences in the CD spectra of 1:1 and 2:1 ratios come from the different CD extrema of d−d transitions of the peptides of His96 and His111. For example, the 4N complex of the peptide Ac-MKHM-NH_2 including His111 is characterized by positive (652/+1.27) and negative (494/−1.56) Cotton

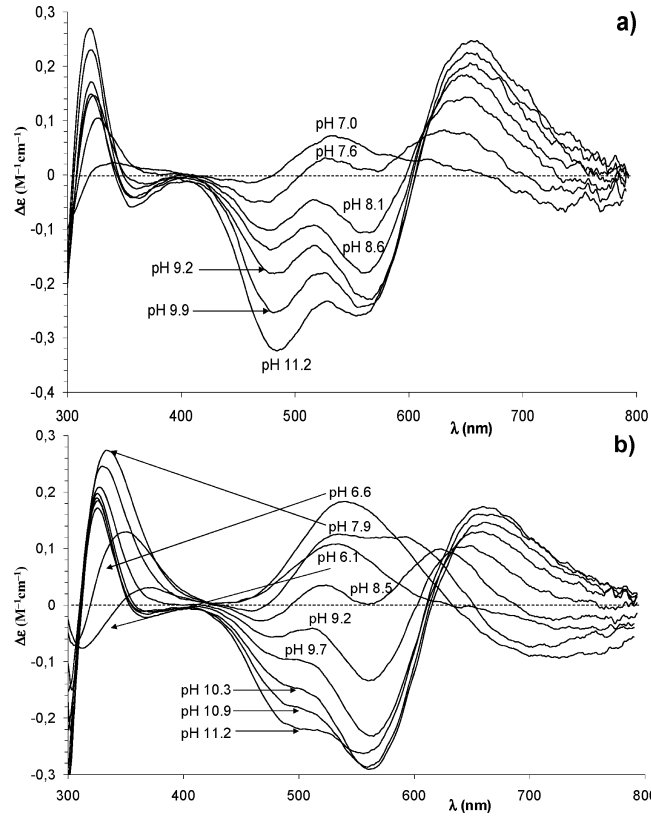

Figure 4. Visible CD spectra of d−d transitions of copper(II) complexes of HuPrP(76−114) at different metal ion-to-ligand ratios and pH values: (a) 1:1 ratio, $c_{copper(II)} = 0.77 \times 10^{-3}$ mol dm^{-3}, $c_L = 0.73 \times 10^{-3}$ mol dm^{-3}; (b) 3:1 ratio, $c_{copper(II)} = 2.07 \times 10^{-3}$ mol dm^{-3}, $c_L = 0.68 \times 10^{-3}$ mol dm^{-3}.

effects in the visible range, while negative (590/−1.93) and positive (495/+1.36) bands are characteristic of Ac-GTHS-NH_2 corresponding to His96.[27] The comparison of CD spectra in Figure 4 clearly indicates that His111 is the major metal binding site in equimolar samples of copper(II) and HuPrP(76−114), while His96 and His111 have almost the same metal ion occupancy at 2:1 ratios. It is clear that the formation of tri- and tetranuclear complexes has only a slight influence on the CD spectra. It is due to the much lower intensity of the CD spectra of octarepeat monomers and reveals that the third and fourth metal ions occupy the octarepeat binding sites.

Potentiometric titration curves reveal that HuPrP(76−114) can keep 4 equiv of metal ions in solution, and precipitation was not observed at any pH values at the ratios from 1:1 to 4:1. This is indirect proof for the formation of polynuclear species in solution, and both computer calculation of potentiometric data and spectroscopic measurements support this assumption. Figures 1 and 2 demonstrate that the dinuclear complexes are present even in equimolar samples, while the polynuclear species predominate at a 3:1 ratio. Similar findings have already been reported for the speciation of the copper(II)−HuPrP(84−114) system, and it was also emphasized that the presence of oligonuclear species in equimolar samples does not necessarily indicate cooperativity in metal binding but can be the result of statistical distribution of the metal ions among the independent binding sites of a polydentate ligand. In the case of HuPrP(76−114), all four

Table 4. Statistical Distribution of Copper(II) Ions in the Various Forms of Oligonuclear Complexes in the Copper(II)−HuPrP(76−114) System Assuming That All Histidine Residues of the Peptide Are Equivalent[a]

	L/M			
complex	1/1	1/2	1/3	1/4
mononuclear	27/64 (42.19%)	1/8 (12.50%)	1/64 (1.56%)	0 (0%)
binuclear	27/64 (42.19%)	3/8 (37.50%)	9/64 (14.06%)	0 (0%)
trinuclear	9/64 (14.06%)	3/8 (37.50%)	27/64 (42.19%)	0 (0%)
tetranuclear	1/64 (1.56%)	1/8 (12.50%)	27/64 (42.19%)	1.00 (100%)

[a] The values represent the mathemathical distribution and percentage of copper(II) among the various oligonuclear species.

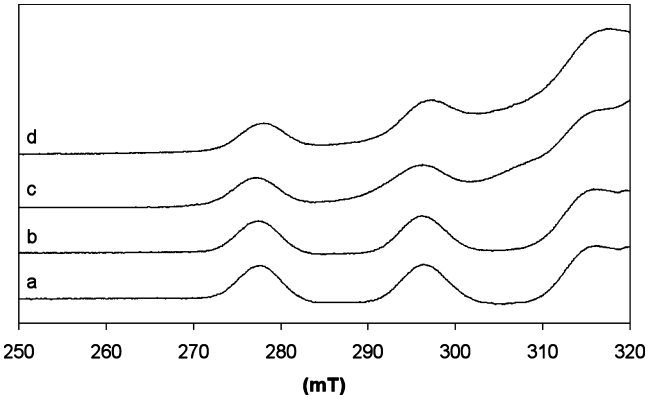

Figure 5. Low-field parallel region of the X-band anisotropic EPR spectra of the $^{63}Cu^{II}$ complexes of HuPrP(76−114) measured at different ligand-to-metal ratios (1 mM $^{63}Cu^{II}$): (a) L/M = 1/1, pH 11.80; (b) L/M = 1/2, pH 11.90; L/M = 1/3, pH 10.30; L/M = 1/4, pH 11.50.

histidyl residues can be metal binding sites and the statistically calculated distribution of copper(II) among these sites is shown in Table 4.

A comparison of Figure 1 and Table 4 reveals a significant difference in the ratio of mono- and dinuclear complexes. The formation of mononuclear species is remarkably favored over that of the dinuclear complexes in the distribution diagram showed in Figure 1. However, it should be considered that the values in Table 4 represent an ideal distribution when all binding sites of the ligand are equivalent. The different ratios of the coordination isomers of mononuclear species have already demonstrated the nonequivalency of these sites, as it was discussed in the previous paragraphs. Even in this case, the overall concentration of the dinuclear species (<10%) is surprisingly low, and it definitely rules out any kind of cooperativity in the binding of the first two metal ions. Spectroscopic measurements provide further support for these findings. There is a sort of correspondence in the UV−vis absorption of 1:1 and 2:1 samples at the same pH values, but the intensities of absorption maxima are doubled or tripled, supporting that all metal ions are present in similar coordination environments. The same increase of the intensity was characteristic of the CD spectra (see Figure 4) with the concomitant change of the positions of CD extrema due to the different metal ion occupancies of the different histidyl binding sites. Figure 5 is used to show the EPR spectra of high-pH samples recorded at four different copper(II) ion-to-ligand ratios. The similarity of the spectral parameters of the 1:1 and 2:1 samples is the most striking in this case and rules out any direct interaction between the copper(II) ions in the dinuclear complexes.

Further evidence for the formation of di-, tri-, and tetranuclear species at any metal-to-ligand ratios was, however, obtained from the ESI-MS measurements (data not shown). The multinuclear species were detected only at pH ≥5.5, indicating that their formation is mainly related to the amide nitrogen deprotonation. Although the spectra were affected by a high noise-to-signal ratio, the changes of the peaks attributed to different species clearly indicate that multinuclear complex species formation is favored with increasing pH values.

His111 and His96, Favored Binding Sites for Copper(II) in Comparison to the Two Histidines of the Octarepeat Region. The data of Table 4, representing the statistical distribution of copper(II) among the equivalent binding sites, indicate that tri- and tetranuclear complexes must predominate in the samples with a 3:1 metal-to-ligand ratio. On the contrary, Figure 2 shows that trinuclear species are present in measurable concentrations only in the physiological pH range (pH 6−8), while the tetra- and dinuclear species predominate in the more alkaline samples. It is the most surprising result of this study and seems to support cooperativity in the binding of the third and fourth metal ions at basic pH values. From evaluation of the CD spectra, we have already concluded that His111 and His96 have higher metal binding affinities than those of His77 and His85 from the octarepeat domain. As a consequence, the first two metal ions in a dinuclear species bind to the histidines outside the octarepeat domain and the dinuclear complexes are mainly characterized by His111 and His96 binding, while the third copper(II) ion can occupy only one of the octarepeat sites. Figure 2, however, reveals that such a species exist only between pH 6 and 8, where the (N_{im},$2N^-$)-coordinated 3N complexes predominate. This binding mode also makes it possible that the fourth coordination site is occupied by the fourth histidyl residue in the form of a macrochelate, and it contributes to the stabilization of the trinuclear complex (see Scheme 1f). Of course, this interaction shifts the deprotonation of the third amide function to a slightly higher pH range. Visible and CD spectroscopic measurements support this assumption because in equimolar samples spectral changes cannot be observed at all above pH 10, while this pH range is continuously shifted to pH 10.5−11 by the increase of the metal ion content of the samples. The exact deprotonation constants of the amide functions, however, cannot be calculated because the deprotonations of amide groups and lysyl side chains significantly overlap in this pH range. Binding of the fourth metal ion disrupts the macrochelate of the trinuclear species, but it can create a weak interaction between the copper(II) ions coordinated in the octarepeat domain. This is reflected in the high-pH EPR spectra as shown by Figure 5. The two spectra measured with 1:1 and 2:1 ratios show a flat baseline, while those measured with 3:1 and 4:1 ratios show that superimposed to the signal due to the monomeric species there is a broad unresolved band. Because we previously measured the shorter fragment HuPrP(84−114) containing only one oct-

arepeat monomer and we did not observe these differences in that case, we have to suppose that this is due to the presence of the two octarepeat fragments. Potentiometric data show that with a 3:1 ratio the trinuclear complexes are not favored: binuclear or tetranuclear complexes are predominantly formed. This means that when 3 equiv of copper are present in solution, the two octarepeat fragments are both involved in the metal coordination or they are not involved at all (see Scheme 1g,h). When both of them are involved in the metal coordination, there is some interaction between the two metal ions, originating the appearance of the broad band. However, there is no significant signal intensity decrease, and this probably means that only in some conformations is there interaction between the two copper ions. In the 4:1 ratio, the line width is increased in comparison with 1:1 and 2:1 ratios. So, the preferred coordination sites are His96 and His111, while His77 and His85 are less favored and show some degree of cooperativity because both or none are involved in the copper binding at basic pH alone, where the 4N complex species (N_{im},$3N^-$) prevail. The preferred coordination for His96 and His111 in comparison with that at His77 and His85 can be rationalized considering that, for the first two sites, in the complexes formed at high pH values with (N_{im},N^-,N^-,N^-) coordination, (5,5,6)-membered joint-chelated rings are formed, while for the two octarepeat residues, (7,5,5)-membered joint-chelated rings are originated. In the 4:1 ratio, the line width is increased in comparison with 1:1 and 2:1 ratios, and this can be explained considering that for the four binding sites the spectral parameters are very similar to each other but not exactly coincident.

Far-UV CD spectra gave further support for the existence of cooperativity above the physiological pH. The HuPrP(84−114) and HuPrP(76−114) peptides adopt predominantly a random-coil conformation[41] (Figures 6 and 7).

Copper(II)-Driven Conformational Changes of the Peptide. Changes in the far-UV CD spectrum of the peptide HuPrP(76−114) were observed upon the addition of increasing amounts of copper(II) at pH 9, where the 4N complex species (N_{im},$3N^-$) form and di- and tetranuclear species formation is favored over the trinuclear complexes especially at a 3:1 metal-to-peptide ratio. Figure 6 shows a reduction in the negative ellipticity at ≈200 nm and an increase in the negative CD band at ≈220 nm, while the inset shows the difference spectra obtained by subtracting the apo-peptide far-UV CD bands. A similar behavior was shown by the HuPrP(84−114) peptide (Figure 7). These spectral changes suggest that copper(II) coordination may induce the formation of turns or structured loops, as was previously reported for the HuPrP(58−91)[11,15] peptide. The CD spectrum of the tetraoctarepeat peptide is characterized by a broad maximum between 225 and 230 nm and a minimum at around 200 nm, indicating a type II poly(L-proline) conformation.[42] When

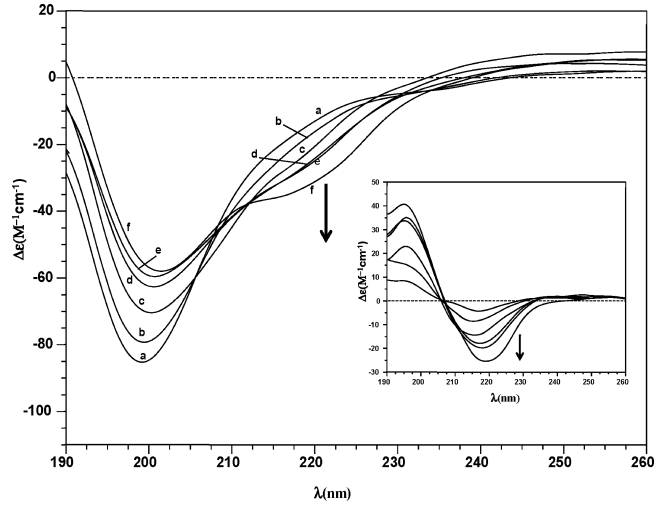

Figure 6. CD spectra of HuPrP(84−114) ($c_L = 1 \times 10^{-4}$ mol dm^{-3}, pH 9) at different concentrations of copper(II)−HuPrP(84−114): (a) $c_{copper(II)} = 0$; (b) $c_{copper(II)} = 3 \times 10^{-5}$ mol dm^{-3}; (c) $c_{copper(II)} = 9 \times 10^{-5}$ mol dm^{-3}; (d) $c_{copper(II)} = 1.6 \times 10^{-4}$ mol dm^{-3}; (e) $c_{copper(II)} = 2 \times 10^{-4}$ mol dm^{-3}; (f) $c_{copper(II)} = 3 \times 10^{-4}$ mol dm^{-3}. Inset: Difference spectra after subtraction of the apo peptide. Arrows indicate curve changes at different concentrations of copper(II).

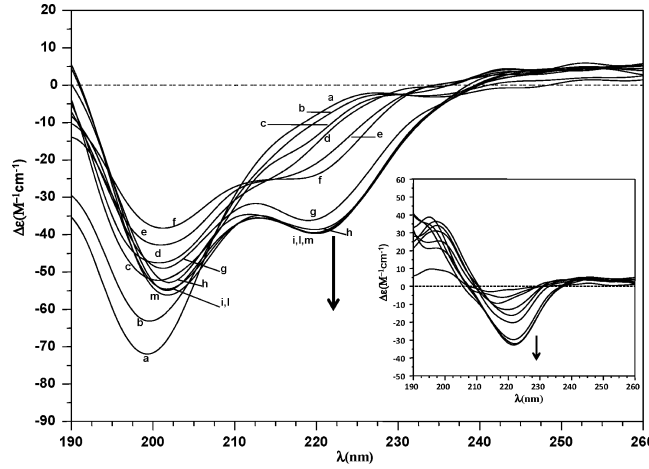

Figure 7. CD spectra of HuPrP(76−114) ($c_L = 3 \times 10^{-5}$ mol dm^{-3}, pH 9) at different concentrations of copper(II)−HuPrP(76−114): (a) $c_{copper(II)} = 0$; (b) $c_{copper(II)} = 1 \times 10^{-5}$ mol dm^{-3}; (c) $c_{copper(II)} = 2 \times 10^{-5}$ mol dm^{-3}; (d) $c_{copper(II)} = 3 \times 10^{-5}$ mol dm^{-3}; (e) $c_{copper(II)} = 4 \times 10^{-5}$ mol dm^{-3}; (f) $c_{copper(II)} = 5 \times 10^{-5}$ mol dm^{-3}; (g) $c_{copper(II)} = 6 \times 10^{-5}$ mol dm^{-3}; (h) $c_{copper(II)} = 8 \times 10^{-5}$ mol dm^{-3}; (i) $c_{copper(II)} = 10 \times 10^{-5}$ mol dm^{-3}; (l) $c_{copper(II)} = 11 \times 10^{-5}$ mol dm^{-3}; (m) $c_{copper(II)} = 12 \times 10^{-5}$ mol dm^{-3}. Inset: Different spectra after subtraction of the apo peptide. Arrows indicate curve changes at different concentrations of copper(II).

increasing equivalents of copper(II) at pH 7.4, where the 3N complex species (N_{im},$2N^-$) prevails, were added, a reduction of the negative band at 200 nm, the development of a positive band at 204 nm, and an increase of the negative ellipticity at 222 nm were observed. The authors proposed that octarepeats are not isolated from each other, but the main chains fold together to produce cooperative binding in the presence of at least two octapeptides.[15]

Interestingly, the $(\Delta\epsilon)_{222}$ values plotted as a function of the Cu/L ratio at pH 9 (Figure 8) for HuPrP(76−114) indicated no spectroscopic change above a 3:1 metal-to-ligand ratio; this behavior is reminiscent of the one reported for the copper(II)−HuPrP(58−91) system.[11,15] This analogy

(41) Kallenbach, N. R.; Lyu, P. C.; Zhou, H. In *Circular Dicroism and the Conformation Analysis of Biomolecules*; Fasman, G. D., Ed.; Plenum: New York, 1996.

(42) Smith, C. J.; Drake, A. F.; Bamfield, B. A.; Bloomberg, G. B.; Palmer, M. S.; Clarke, A. R.; Collinge, J. *FEBS Lett.* **1997**, *405*, 378–404.

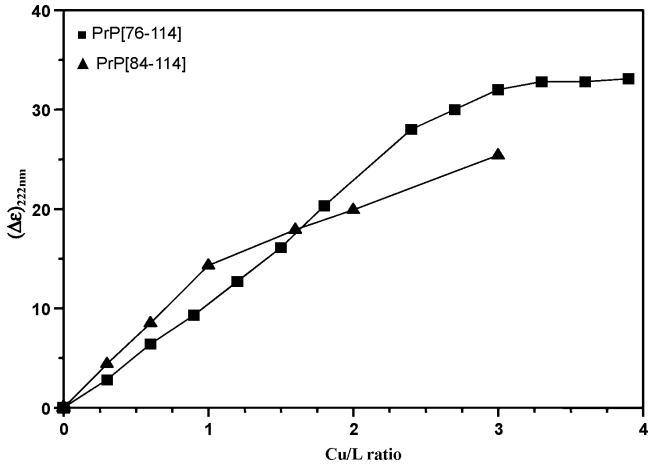

Figure 8. $(\Delta\epsilon)_{222}$ of HuPrP(76−114) (pH 9) and HuPrP(84−114) (pH 9) at different metal-to-peptide (L) ratios.

further indicates that the third and fourth copper(II) equivalents occupy the octarepeat binding sites of HuPrP(76−114). Moreover, when the $(\Delta\epsilon)_{222}$ values are plotted as a function of the Cu/L ratio at pH 9 for the copper(II)−HuPrP(76−114) and copper(II)−HuPrP(84−114) systems, it turns out that spectral changes are more pronounced in the first system, suggesting that the presence of a single octarepeat sequence does not bring any cooperative effect in the coordination of copper(II) with the peptide.

Conclusions

Since the discovery of the physiological link between PrP and the copper(II) ion,[3,11,15,43] there have been a large number of investigations to elucidate the role of copper(II) in prion protein's function,[44] attempting to define the copper(II) coordination environments,[16] and to determine the precise affinity for metal ion binding to PrP.[19,35] The large discrepancies reported for the affinity of copper(II) interactions with full-length PrP, with values ranging between micromolar[3,45] and femtomolar,[34,46] motivated the need to obtain reliable affinity values of the protein for copper(II) and the metal ion coordination modes of the different species formed both at different pH values and at various copper(II) to full-length prion ratios. Though previous and recent findings provide evidence that the binding sites for copper(II) to the full-length protein and to its peptide fragments are the same,[11,35] the use of different peptide fragments did not prevent the indication of the affinity in terms of estimated K_D values.[19,35] A large body of literature,[7,14,17,18,23,24,28,29,32] together with our current work, now exists that demonstrates, by means of potentiometric measurements, that a number of overlapping copper(II) complexes with prion peptide fragments form in the same pH range. These findings that stress the need to obtain a detailed speciation can explain the wide disagreement of the affinity values. To partly mimick the metal ion interactions with the unstructured domain of prion protein, HuPrP(23−125), a combination of potentiometric and various spectroscopic techniques (UV−vis, CD, ESR, and MS) was used to determine the metal ion speciation and structures of the major species formed in the copper(II)−HuPrP(76−114) system. The results show that the complex formation of the metal ions starts in a slightly acidic pH range (pH ∼3) and completes by the physiological pH. Imidazole nitrogen donor atoms are the primary and exclusive metal binding sites below pH 5.5 in the form of various macrochelates. The overall stability constants of these macrochelates are listed in Table 3, and the data reflect the increasing stability by the increasing number of coordinated nitrogen donors. Other research groups have found evidence for the coordination of a single copper(II) ion by multiple histidine imidazoles at low peptide to copper(II) ratios, using peptide fragments encompassing the octarepeat region.[16,37] All six N-terminal histidine residues (the four from the octarepeat region and two, His96 and His111, from the domain in between the OR region and the structured C terminal) contribute to the coordination of the two copper(II) ions.[38] These findings are in agreement with our results. In the main metal complex species formed at pH 6 (i.e., $[CuH_4L]$ Figure 1), a macrochelate forms thanks to the histidine imidazole coordination and is characterized by the four histidine coordination (Scheme 1a). The macrochelation slightly delays, but cannot prevent, the deprotonation and metal ion coordination of amide functions, resulting in the formation of (N_{im},N^-), (N_{im},N^-,N^-), and (N_{im},N^-,N^-,N^-) or, in other words, 2N-, 3N-, and 4N-coordinated copper(II) complexes in the pH range from 5.5 to 9. Spectroscopic measurements provide unambiguous proof for the increasing number of nitrogen donors in these species. A further increase of the pH, however, does not result in any spectral changes, supporting that the lysyl side chain amino groups are not metal binding sites. An important difference in the metal ion coordination of amide groups of HuPrP(76−114) and its short counterparts [e.g., HuPrP(94−97) and HuPrP(109−112)] is reflected in the lack of cooperativity for amide deprotonation processes with HuPrP(76−114). It can probably be explained by the metal ion coordination of distant histidyl residues in the 3N complexes, suggesting that macrochelation enhances the thermodynamic stabilities of these species, too.

The application of CD spectroscopy provided clear evidence that all histidyl residues can be metal binding sites, and this results in the existence of coordination isomers of all possible species. The nonequivalency of the histidyl binding sites was unambiguously proved for the small fragments of the protein, and the same trends were found for the four-histidine peptide, HuPrP(76−114), too. The metal binding affinity of the histidyl sites follow the order His111 > His96 ≫ His77 ∼ His85 [the latter two histidines are from the octarepeat region, and we cannot differentiate between their copper(II) binding affinities because they have the same amino acid sequences]. Figure 9 demonstrates the metal ion distribution of a model system when the bis-

(43) Pan, K. M.; Stahl, N.; Prusiner, S. *Protein Sci.* **1992**, *1*, 1343–1352.
(44) Davies, P.; Brown, D. R. *Biochem. J.* **2008**, *410*, 237–244.
(45) Kramer, M. L.; Kratzin, H. D.; Schmidt, B.; Romer, A.; Windl, O.; Liemann, S.; Ornemann, S.; Kretzschmar, H. *J. Biol. Chem.* **2001**, *276*, 16711–16719.
(46) Jackson, G. S.; Murray, I.; Hosszu, L. L. P.; Gibbs, N.; Waltho, J. P.; Clarke, A. R.; Collinge, J. *Proc. Natl. Acad. Sci. U.S.A.* **2001**, *98*, 8531–8535.

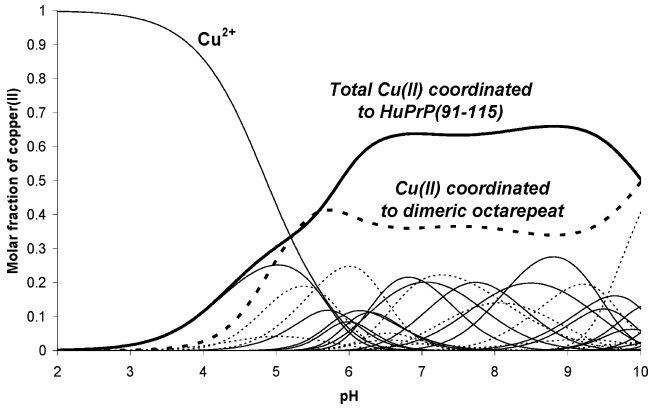

Figure 9. Distribution of copper(II) among the peptides bis-octarepeat[18] and HuPrP(91−115)[30] at a 2:1:1 ratio. $c_{\text{copper(II)}} = 2 \times 10^{-3}$ mol dm^{-3}, and $c_{\text{bis-octarepeat}} = c_{\text{HuPrP(91-115)}} = 1 \times 10^{-3}$ mol dm^{-3}. The bold line indicates the sum of the complex species of the copper(II)−PrP(91−115) system. The dashed line indicates the sum of the complex species of the copper(II)−bis-octarepeat system.

octarepeat[18] and the peptide HuPrP(91−114) outside the octarepeat region[32] are present in equimolar concentration. Both bis-octarepeat and HuPrP(91−114) contain two histidines. It is clear from Figure 9 that the affinities of copper toward the two histidines outside and inside the octarepeat region are very much comparable under slightly acidic (pH 5−6) and strongly basic (pH >10) conditions. At the same time, in the neutral or physiological pH ranges, the affinities of copper(II) toward the two histidines outside the octarepeat region are higher, even in the presence of a bis-octarepeat.

The major effect of the presence of four histidyl residues is reflected in the high tendency of HuPrP(76−114) to form oligonuclear complexes. Among them, the formation of di- and tetranuclear species seems to be favored over the trinuclear ones, at basic pH values. This phenomenon was not observed in the complex formation reactions of HuPrP(84−114) containing only one histidyl residue from the octarepeat.

Acknowledgment. This work was supported by the Hungarian Scientific Research Fund (OTKA T048352), by the MTA (Hungary)−CNR (Italy) bilateral program, and by MIUR (FIRB RBNE03PX83).

Supporting Information Available: Visible CD spectra of d−d transitions of copper(II) complexes of HuPrP(76−114) at 1:2 and 1:4 ion-to-ligand ratios, respectively. This material is available free of charge via the Internet at http://pubs.acs.org.

IC802190V